A GENERAL MODEL FOR RAYLEIGH WAVE - SURFACE FEATURE SCATTERING PROBLEMS

R.J. Blake

SERC Daresbury Laboratory
Daresbury, Warrington WA4 4AD, U.K.

L.J. Bond

Department of Mechanical Engineering
University College London
Torrington Place, London WC1E 7JE, U.K.

INTRODUCTION

In non-destructive testing, it has been suggested that wavelength or frequency dependent Rayleigh wave scattering coefficients could provide a means of characterising surface defects. Only a few Rayleigh wave scattering problems have analytic solutions and most workers have resorted to numerical techniques [1]. In this paper we present details of a new model that can deal with general surface defect geometries. The scheme is used to model Rayleigh wave scattering from curved corners, steps and slots. The implications of the results for a Rayleigh wave based defect characterisation method are discussed briefly.

NUMERICAL MODEL

To date, most numerical solutions of the time dependent plane strain elastic equations of motion have been restricted to simple geometries. The time derivatives are usually approximated by an explicit algorithm, and for stable solutions the time increment is limited by the smallest grid increment used in the spatial discretisation. Complicated geometries often demand irregular, high resolution, spatial grids and consequently small time increments have to be used. The large number of time steps needed to evolve these geometries makes explicit schemes very expensive. The usual way to overcome stability problems is to use an implicit scheme to effect the temporal discretisation. The displacements at a future time level are calculated for all the spatial nodes by solving a set of simultaneous linear equations. However, for large scale models this proves to be prohibitively expensive. An economic solution can be calculated if we use an explicit temporal scheme for the majority of spatial nodes defined on a regular spatial grid which surrounds an irregular spatial grid containing the surface feature, where an implicit temporal scheme is used. Such mixed explicit-implicit time schemes can also be used to overcome stability problems in multi-media models [2].

We have developed a general model for Rayleigh wave scattering problems which is illustrated in Fig. 1. As usual, the geometry is restricted to two spatial dimensions. Bilinear displacement quadrilateral, and linear displacement triangular, finite elements are used to effect the spatial discretisation in both the regular and irregular regions. A lumped mass matrix and the centred difference quotient are used to advance the solution in the regular region of the grid. This algorithm is far more accurate than commonly

Review of Progress in Quantitative Nondestructive Evaluation, Vol. 9
Edited by D.O. Thompson and D.E. Chimenti
Plenum Press, New York, 1990

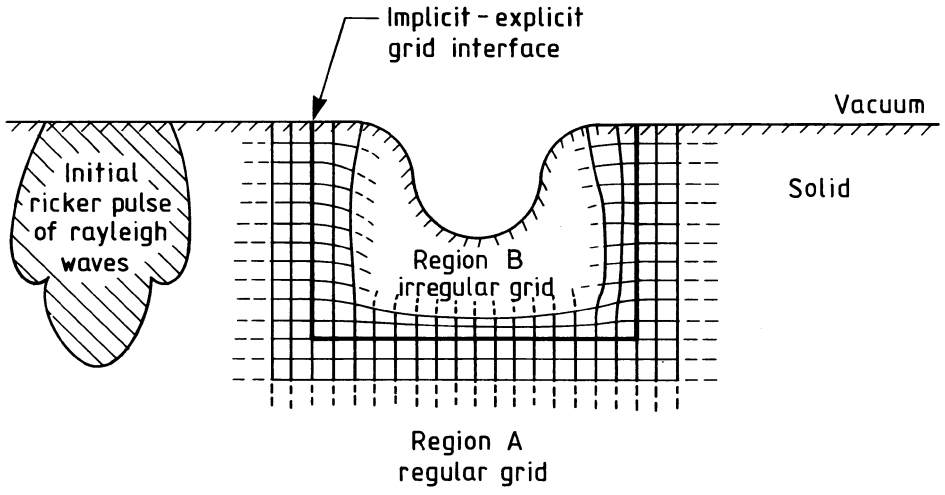

Fig. 1. Mixed implicit-explicit/irregular-regular grid numerical model.

used finite difference schemes [1,3]. In the irregular grid region, the consistent form of the mass matrix is retained and the implicitly stable Newmark algorithm is used to advance the solution. The initial conditions for the model involve specifying the Rayleigh wave pulse in a limited region of space in the regular part of the grid at two time levels. The explicit algorithm is then used at all points in the regular grid. The new displacements at nodes in the regular grid adjacent to the irregular grid act as boundary conditions for the implicit equations which are solved using the Incomplete Cholesky Conjugate Gradient method. The time indices are then cycled and the solution is evolved.

The new model has been tested by solving the problem of Rayleigh wave propagation along a half space. The Ricker pulse of Rayleigh waves is characterised by a central wavelength λ_0 which is used to define the spatial grid. Typically we use a regular grid increment of $d = \lambda_0/48$ in both directions and a temporal increment of $s = 0.9\ d/V_C$ to advance the solutions in both of the grids. Regular grid dimensions of 1001 by 2001 nodes and irregular grid dimensions of 101 by 201 nodes are evolved for about 1500 iterations. In this paper we consider material parameters for mild steel: $V_C = 5960$ m/s, $V_S = 3235$ m/s and $V_T = 2995$ m/s. Fig. 2 shows the amplitude errors in the vertical component of displacement at the surface, after the Ricker pulse has propagated through a regular or typical irregular implicit grid embedded in a half space. As the wavelength decreases the amplitude errors increase quadratically being of order 0.25% for $\lambda = \lambda_0$ and 1% for $\lambda = \lambda_0/2$. Less than 0.5% of the incident amplitude is reflected by the embedded implicit grid region. There is little difference between the results for the regular or irregular implicit grids and the new model gives results which are almost identical to those of fully explicit models for simple scattering geometries.

RAYLEIGH WAVE SCATTERING FROM CURVED CORNERS

Fig. 3 presents numerical visualisations of Rayleigh waves scattered from 90° corners with radius of curvature $R = 0$ and $R = \lambda_0$. The displacement wavefield is drawn as a

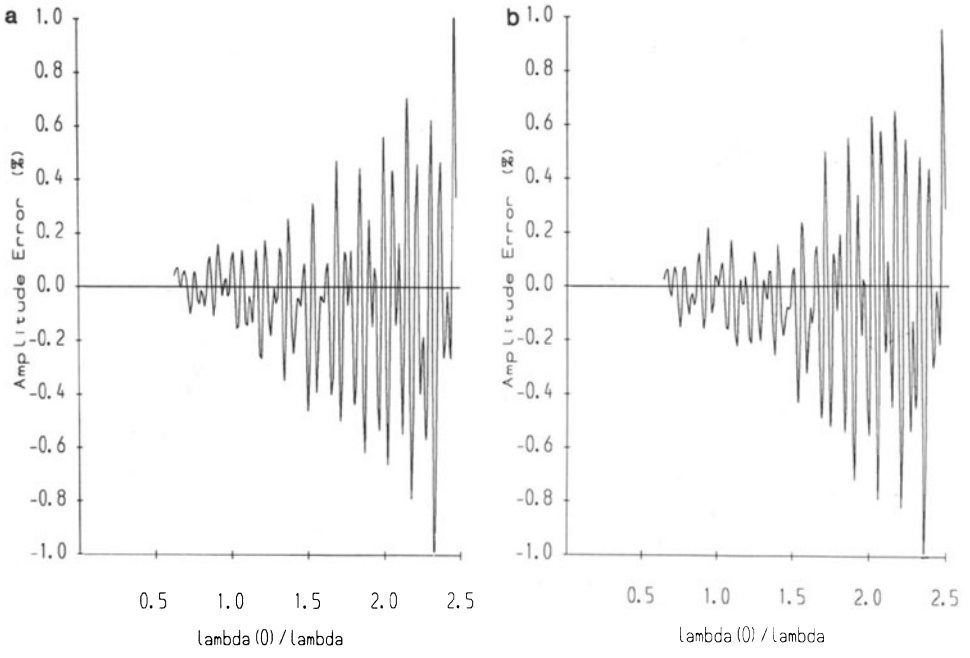

Fig. 2. Errors in Rayleigh wave propagation through (a) regular and (b) irregular grid implicit regions.

small vector from the equilibrium position of a set of the nodes. The amplitude of the reflected Rayleigh wave is smaller, and the amplitude of the transmitted Rayleigh wave is bigger, for the sharp corner. The angular distribution of the body wave pulses changes dramatically. The minimum in the shear wavefield along the wedge bisector in the sharp corner geometry is missing in the curved geometry and the maximum in the compression wavefield moves away from the reflection surface towards the transmission surface. Of course each wavelength in the incident pulse sees a corner with an effective radius of curvature R/λ and responds differently. Naively, one would assume that the shorter wavelengths see a smoother corner and are scattered less. Hence as R/λ increases the reflection coefficient should decrease monotonically to zero and the transmission coefficient should increase monotonically to unity. However, this is not the whole story as can be seen from the wavelength dependent Rayleigh wave scattering coefficients presented in Fig. 4. Data derived from models with different R are accumulated into a single graph, the width of the plots illustrates that the errors in the scattering coefficients are of order $\pm$ 1%. For small values of R/λ the scattering coefficients converge to the sharp corner values obtained from fully explicit models [3]. In the region of large R/λ values the simple picture of diminishing reflection coefficient and increasing transmission coefficient is valid. However, in the middle range of R/λ values, the variation of the scattering coefficients with R/λ is reminiscent of the obtuse wedge geometry [3]. As the internal wedge angle increases from 90° to 180° the reflection coefficient first of all increases then decreases to zero. The transmission coefficients have the opposite behaviour. This leads us to conjecture that the main source of the scattered wavefield is localised and located some way down the transmission surface. As the wavelength incident upon the curved corner decreases, the effective source of the scattered wavefield moves off the vertical surface onto the curved surface. Locally this source point sees a sloping surface whose angle to the horizontal surface changes from 90° to 180° as the wavelength decreases.

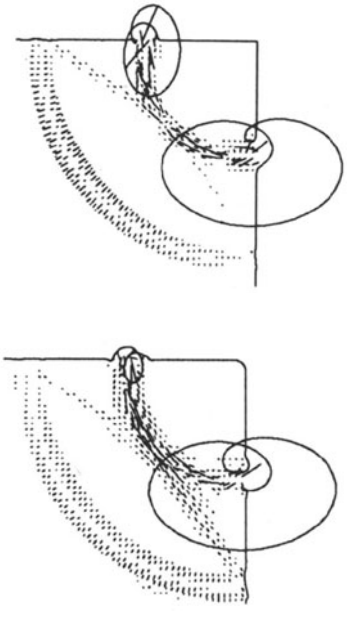

Fig. 3. Rayleigh wavefields scattered from 90° corners.

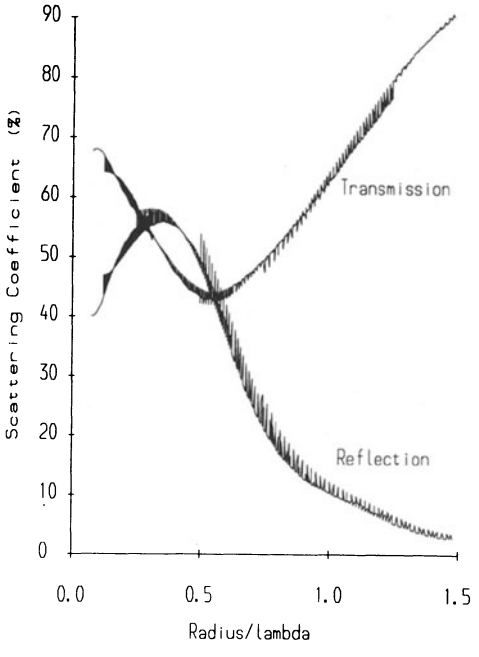

Fig. 4. Rayleigh wave scattering coefficients for curved 90° corners.

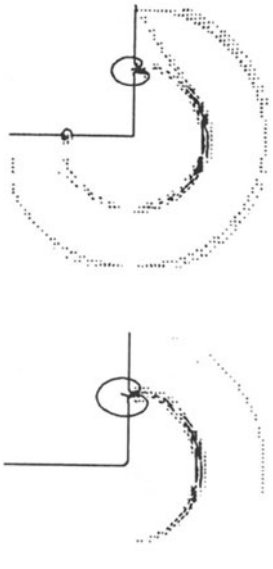

Fig. 5. Rayleigh wavefields scattered from 270° corners.

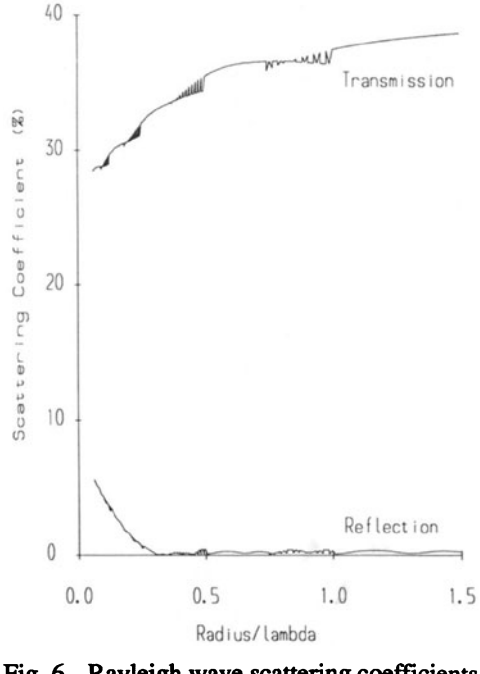

Fig. 6. Rayleigh wave scattering coefficients for curved 270° corners.

The wavefield scattered from 270 degree corners with R = 0 and R = λ_0 is illustrated in Fig. 5. Here the picture is far simpler. As Fig. 6 shows, the reflected Rayleigh wavefield decreases monotonically with increasing ratio of R/λ whereas the transmitted wavefield increases. For small values of R/λ the scattering coefficients converge to the sharp corner values obtained from fully explicit models [3].

RAYLEIGH WAVE SCATTERING FROM CURVED STEPS

Fig. 7 presents numerical visualisations of a Ricker pulse of Rayleigh waves scattered from down steps of depth d = λ_0 with corners of radius of curvature R = 0 and R = d/2. The amplitudes and spatial distribution of both the surface and body waves are very different, illustrating the strong influence that curvature of the defect geometry has on the scattered wavefield. The wavefields beneath the left hand surface are clearly characteristic of the isolated top corner geometry, whereas the transmitted wavefield contains contributions from wavefields generated by the tail of the incident wavefield at the bottom corner and from wavefields transmitted through both the top and bottom corners [3]. Fig. 8 presents wavelength dependent reflection coefficients. For long wavelengths, the reflected wavefield is only sensitive to the step depth. However, the middle frequency and high frequency (large d/λ) response is sensitive to the curvature as well. For sharp corners, we get characteristic oscillations resulting from the interference between waves scattered from the top and bottom of the step. The peak in the isolated curved 90° corner reflection coefficient occurred at R/λ = 0.4. For the step containing corners with R = d/4 this should manifest itself at d/λ = 1.6 as indeed it does. There are no oscillations in this structure because the wavefield reflected from the curved 270° corner at the bottom of the step are negligible. For the step containing corners with R = d/2 there should be a corresponding feature at d/λ = 0.8. The effect is less dramatic because the amplification resulting from the top corner coincides with a minimum resulting from scattering from the step as a whole. In the high frequency regime, the effects of corner curvature take their toll and the reflection coefficients rapidly decrease to zero.

Fig. 9 presents visualisations of Rayleigh waves scattered from up steps of height h = λ_0 with corners of radius of curvature R = 0 and R = h/2. Once again the surface and body wavefields are very different, for the curved step the reflected wavefield is dominated by the reflection from the top corner. Fig. 10 presents the wavelength dependent reflection coefficients. The peak at long wavelengths arises because the bottom corner is the near-field of the amplified wavefields generated at the top corner. This reduction in amplitude in the first peak, as the curvature of the corners increases, mimics the behaviour in angled up step geometries [3]. In the high frequency region (large h/λ) the amplitude reflected from the sharp step oscillates as the wavefields scattered from the top and bottom corners interfere. For the curved geometries practically no amplitude is reflected from the bottom corner and there are no interference effects. The enhanced reflection from the top corner presents itself as a small summit/plateau at h/λ = 1.6 for the R = h/4 up step, and as a shoulder at h/λ = 0.8 in the first peak for the R = h/2 up step. Once again in the high frequency regime, the effects of curvature reduce the reflection coefficients rapidly.

RAYLEIGH WAVE SCATTERING FROM CURVED SLOTS

Fig. 11 presents numerical visualisations of Rayleigh waves scattered from a λ_0 deep $\lambda_0/2$ wide slot with corners of radius of curvature R = 0, and a λ_0 deep $2\lambda_0$ wide slot with corners of radius of curvature R = d/2. The reflected wavefields are very similar to the wavefields reflected from the corresponding down step. Figs. 12, 13 and 14 present the wavelength dependent reflection coefficients for slots with various depth to width ratios. For large d/λ, the reflection coefficients are almost identical to those of the corresponding down step. The weak reflection properties of the up step impose a small modulation on the down step spectra. However, for d/λ or h/λ < 0.5 the scattering from the top

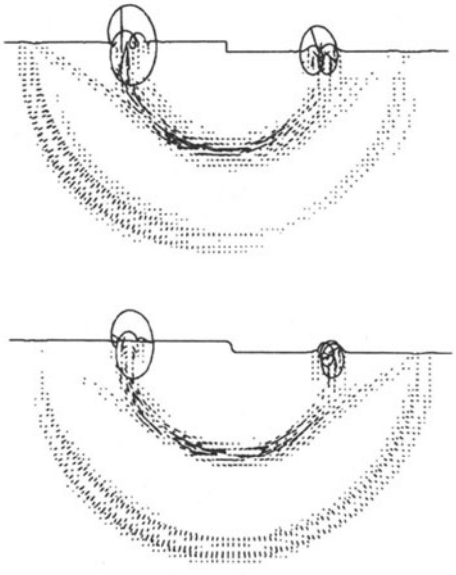

Fig. 7. Rayleigh wavefields scattered from down steps.

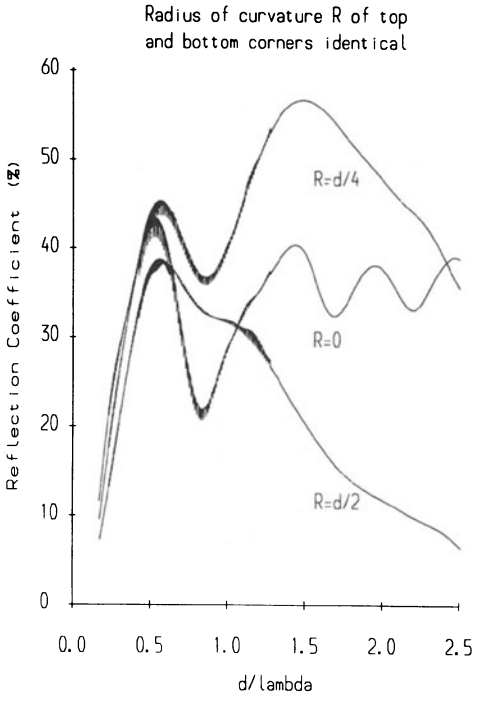

Fig. 8. Rayleigh wave reflection coefficients for curved down steps.

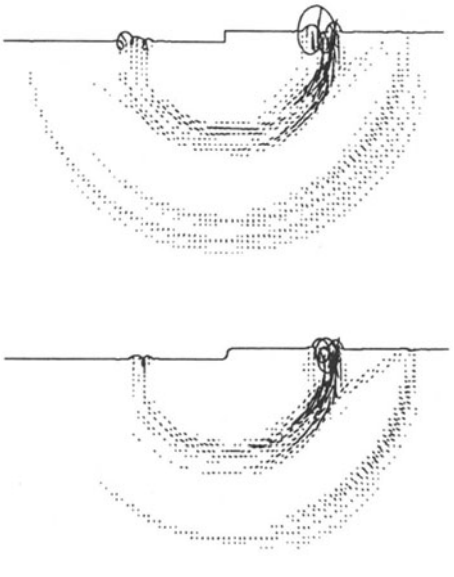

Fig. 9. Rayleigh wavefields scattered from up steps.

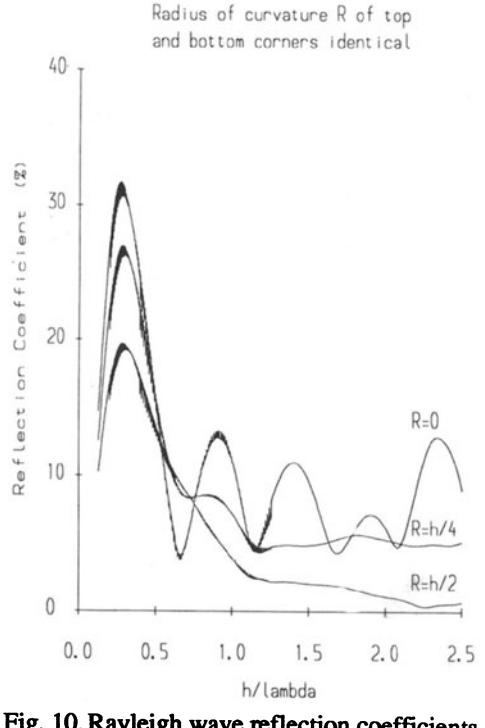

Fig. 10. Rayleigh wave reflection coefficients for curved up steps.

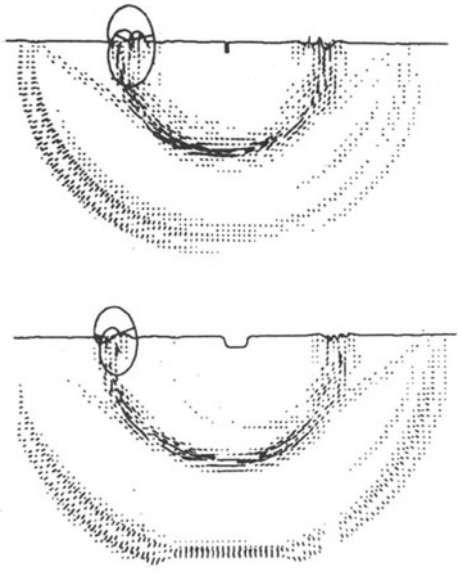

Fig. 11. Rayleigh wavefields scattered from slots.

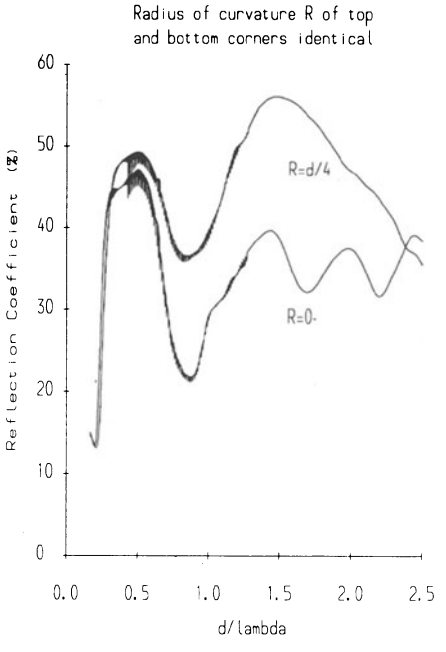

Fig. 12. Rayleigh wave reflection coefficients for curved slots with depth/width = 2.

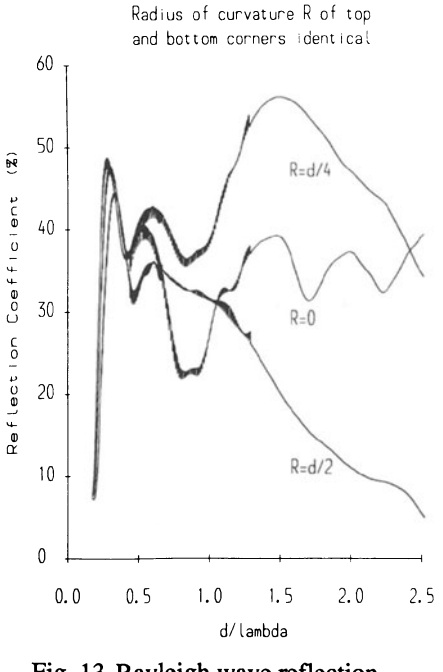

Fig. 13. Rayleigh wave reflection coefficients for curved slots with depth/width = 1.

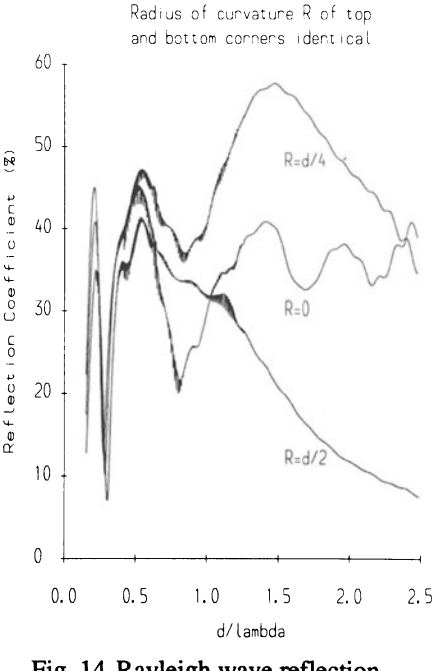

Fig. 14. Rayleigh wave reflection coefficients for curved slots with depth/width = 1/2.

corner of the up step is strong and the up step contributes significantly to the wavefield reflected from the slot. The path length between the wavefields reflected from the up step and down step parts of the slot varies with the width of the slot. For thin slots (depth = 2* width), the path length is short and the up step broadens the first peak in the wavefield reflected from the down step. As the slots get wider, the wavefield separation increases and leads to a modulation of the reflection coefficients. The period of the modulation is inversely related to the path length. For the square slots (depth = width) a peak induced by the up step is split away from the first down step peak. For the fat slots (depth = width/2), the up step induced structure has a correspondingly smaller wavenumber interval. Not only is a peak split off, but shoulders are induced in the main down step peak.

RAYLEIGH WAVE NDT

In the above we have concentrated on the reflected Rayleigh wavefield. Rayleigh wave transmission coefficients are difficult to calculate because of the presence of shear waves radiated from the bottom of the slot onto the transmission surface. As we have shown above, the depth, width and radius of curvature all contribute wavelength dependent features to the reflected wavefield. Given that curvature considerably dampens the high frequency or short wavelength reflection properties of the slot we suggest that a Rayleigh wave NDT method should concentrate on the low to middle wavelength regime. It is noticeable that the amplitude and position of the first down step peak at $d/\lambda = 0.5$ are relatively insensitive to the width and the radius of curvature of the slot. The width of the slot can be deduced by examining the wavenumber interval of structure imposed on the down step peak and finally, the radius of curvature of the corners can be deduced by the presence or absence of high frequency structure. However, we know from our other work [3] that the inclination of the slot surfaces also has a dramatic effect on the reflection coefficients and these effects still have to be included before a viable Rayleigh wave based surface defect characterisation method can be proposed.

REFERENCES

1. R.J. Blake and L.J. Bond, Ultrasonics, in press (1989).
2. T. Belytschko and R. Mullen, Int. J. Num. Meth. Eng. 12, 1575 (1978).
3. R.J. Blake, Ph.D. dissertation, Dept. Electronic and Electrical Engineering, University College London, 1988.